Pergamon

Tetrahedron 56 (2000) 105–119

TETRAHEDRON

2,6-Dimethoxyphenylphosphirane Oxide and Sulfide and their Thermolysis to Phosphinidene Chalcogenides—Kinetic and Mechanistic Studies

Peter P. Gaspar,[a,*] Hu Qian,[a] Alicia M. Beatty,[a] D. André d'Avignon,[a] Jeff L.-F. Kao,[a] Jesse C. Watt[a] and Nigam P. Rath[b]

[a]*Department of Chemistry, Washington University, St. Louis, MO 63130-4899, USA*
[b]*Department of Chemistry, University of Missouri—St. Louis, St. Louis, MO 63121, USA*

Received 10 May 1999; accepted 2 July 1999

Abstract—2,6-Dimethoxyphenylphosphirane is readily converted to its oxide and sulfide whose pyrolysis and (perhaps) photolysis lead to the generation of phosphinidene chalcogenides Ar–P=Z (Z=O,S). Trapping experiments were carried out under conditions similar to the kinetic studies of the phosphirane chalcogenide pyrolyses that confirmed the formation of free Ar–P=Z. The trapping experiments were in accord with carbene-like character for Ar–P=Z, and the activation parameters suggest a non-least motion pathway for the addition of Ar–P=Z to olefins. This represents quantitative evidence for the validity of the predictions of frontier-orbital theory for species that undergo reactions with small (or no) enthalpic barriers.

Introduction

It was recognized several years ago that differences in frontier-orbital symmetry between the 'carbene family' and 'nitrene family' of six-valence electron species might allow a fundamental question regarding chemical reactivity to be answered: does maximization of bonding in the transition state of a reaction, as embodied in frontier-orbital (FO) theory, correctly predict reaction pathways, *even in the absence of a significant energy barrier*?[1] Frontier orbitals of closed-shell singlet silylenes and phosphinidenes, and of a phosphinidene chalcogenide are shown in Scheme 1.[2]

The HOMO of the silylene is aligned with the molecular axis (and the HOMO of the phosphinidene chalcogenide has the same 'local symmetry') while the HOMO of the phosphinidene is perpendicular to the molecular axis. This difference in symmetry will lead to a non-least motion transition state for concerted addition of a silylene or a phosphinidene chalcogenide to an olefin, *if* FO overlap is maximized, but permits a least motion transition state for concerted addition of a phosphinidene. In Scheme 2, orientations of a silylene, phosphinidene and phosphinidene chalcogenide that maximize overlap of their HOMO's with an olefin LUMO are shown at the left. Curved arrows indicate the motions of substituents on a silylene and a phosphinidene chalcogenide necessary to interconnect their positions in the non-least motion transition state with their positions in the corresponding silirane and phosphirane chalcogenide adducts.

It is more than 40 years since Skell proposed that stereospecific addition of carbenes to olefins was due to a concerted process involving a singlet species.[3] It has been pointed out that singlet carbenes or silylenes could undergo stepwise, non-stereospecific addition, and triplet species might add stereospecifically if conformational changes were slow compared with intersystem crossing and intramolecular radical coupling.[4,5] Nevertheless the reactant orientations and transition state structures shown in Scheme 2 should describe the maximization of bonding during concerted addition (and retroaddition) processes of closed-shell singlet species.

In 1963 Moore suggested that concerted addition by a singlet carbene to an olefin implied a maximization of what we now call FO-interactions, half of which are shown in Scheme 2.[6] By 1968 Roald Hoffmann had pointed out that the 'least motion' transition-state for carbene addition was forbidden by symmetry, and he predicted, on the basis of extended-Hückel calculations, that there would be a significant energy barrier along this pathway but none along the non-least motion pathway depicted in Scheme 2.[7] There was no experimental evidence for non-least-motion addition.

There have been many calculations at various levels of theory on the addition of carbenes to olefins,[8] and they are all in accord with Hoffmann's view that a non-least motion

Keywords: phosphorus heterocycles; strained compounds; phosphine oxides; phosphine sulfides.
* Corresponding author. Tel.:+314-935-6568; fax: +314-935-4481; e-mail: gaspar@wuchem.wustl.edu

0040–4020/00/$ - see front matter
PII: S0040-4020(99)00779-6

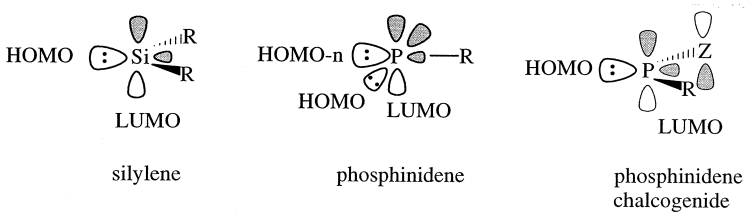

Scheme 1.

pathway is preferred. A similar picture emerges from calculations on the pathways for the silylene–olefin addition reaction. Gordon has predicted that along the minimum energy approach of SiH_2 to ethylene the H–Si–H plane remains parallel to the plane containing the ethylene nuclei until late in the reaction when there is an abrupt change in the angle between the planes, as shown in Scheme 2.[9]

In accord with these theoretical results is the qualitative picture of approach control governed by orbital overlap that emerges from the FO model: HOMO–LUMO mixing lowers the energy of the transition-state, and hence reaction occurs by the pathway that maximizes FO overlap.

To be sure, these are enthalpic considerations, and transition states are related to free energy barriers. Given the tremendous success of FO theory in organic chemistry,[10] it may seem wrongheaded to question its predictive powers in the realm of highly reactive species. But most carbene and silylene reactions are highly exothermic, and laser-flash kinetic spectroscopy has indicated that their addition reactions are very rapid, some occurring at the diffusion-controlled rate. Thus activation barriers are very small, and indeed often *negative*,[11] and little bonding has occurred when the transition state is reached.

Houk has proposed entropic control of the free energy barrier for carbene addition reactions.[12] A consequence of entropic rather than enthalpic control of addition rates would be that maximization of bonding, an enthalpic factor, might fail as a predictive model for transition state structure.

The non-least motion transition states predicted by the FO model, and supported by calculations of minimum energy pathways, for addition reactions of the 'carbene family' should lead to a lower entropy of activation than would a least-motion transition state for both the forward and reverse reactions. This is due to the 'extra' steric interactions between substituents on the olefin and those on the attacking species that are not present in the adduct or the free reagents.

We favor kinetic studies of the retro-additions, shown in cartoon form in Scheme 3, because their reasonably large activation barriers considerably ease the task of measuring their rates and of obtaining their activation parameters from the temperature dependence of their rate constants. The addition (and indeed all other) reactions of silylenes have been found to be cleanly reversible,[13] and this prompted us to develop the

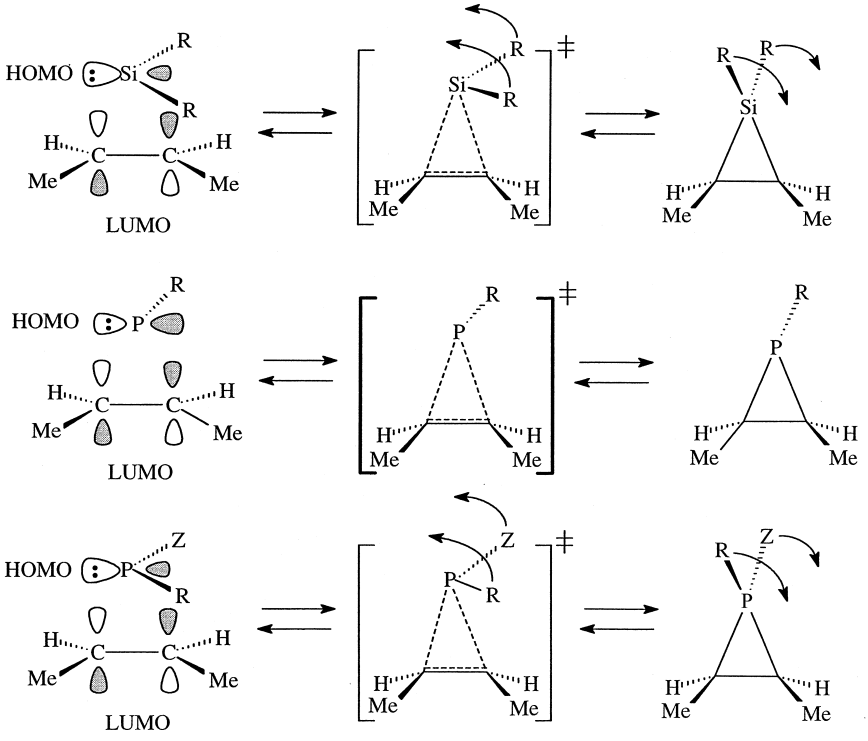

Scheme 2.

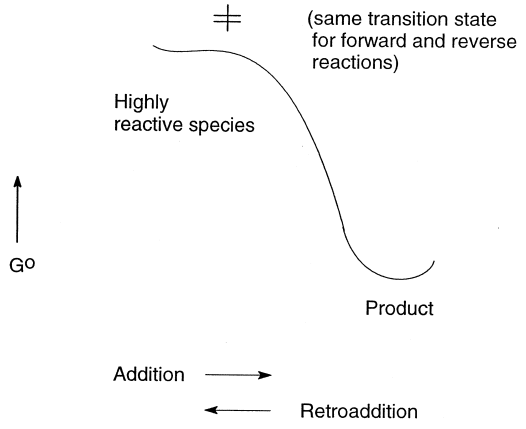

Scheme 3.

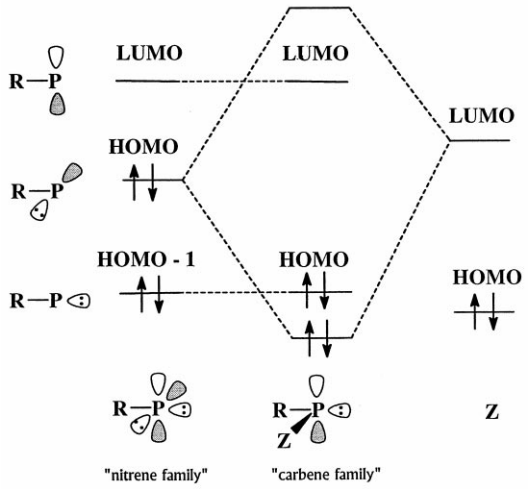

Scheme 4.

retroaddition route to phosphinidenes.[14] Arylphosphiranes have been found to undergo clean pyrolysis and photolysis to phosphinidenes R–P.[15]

Our interest in phosphinidene chalcogendides R–P=Z (Z=O, S, Se, Te) has been kindled by the recognition that conversion of R–P to R–P=Z changes the symmetry of the HOMO making R–P=Z isolobal with a singlet carbene or silylene.[16] This is shown in Scheme 4 in an MO interaction diagram.

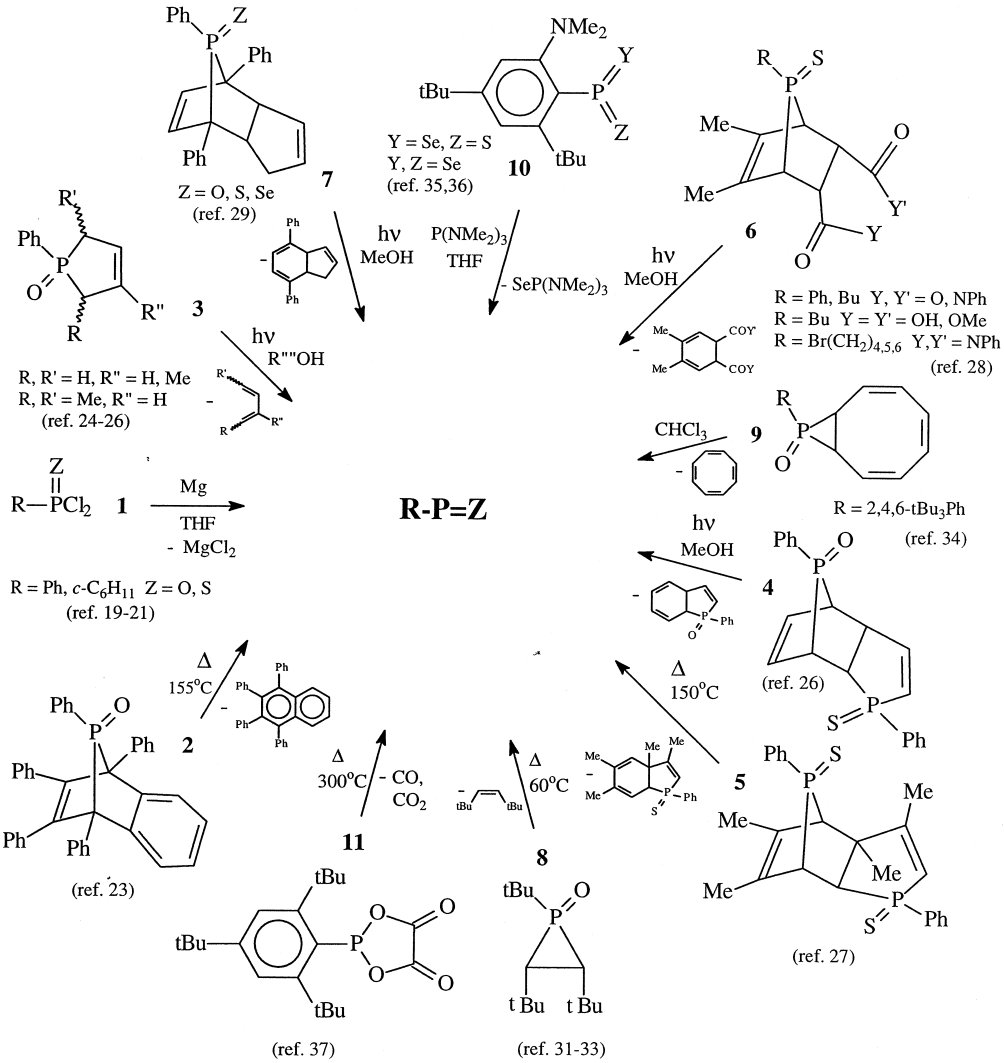

Figure 1. Reactions that have been reported to yield phosphinidene chalcogenides R–P=Z.

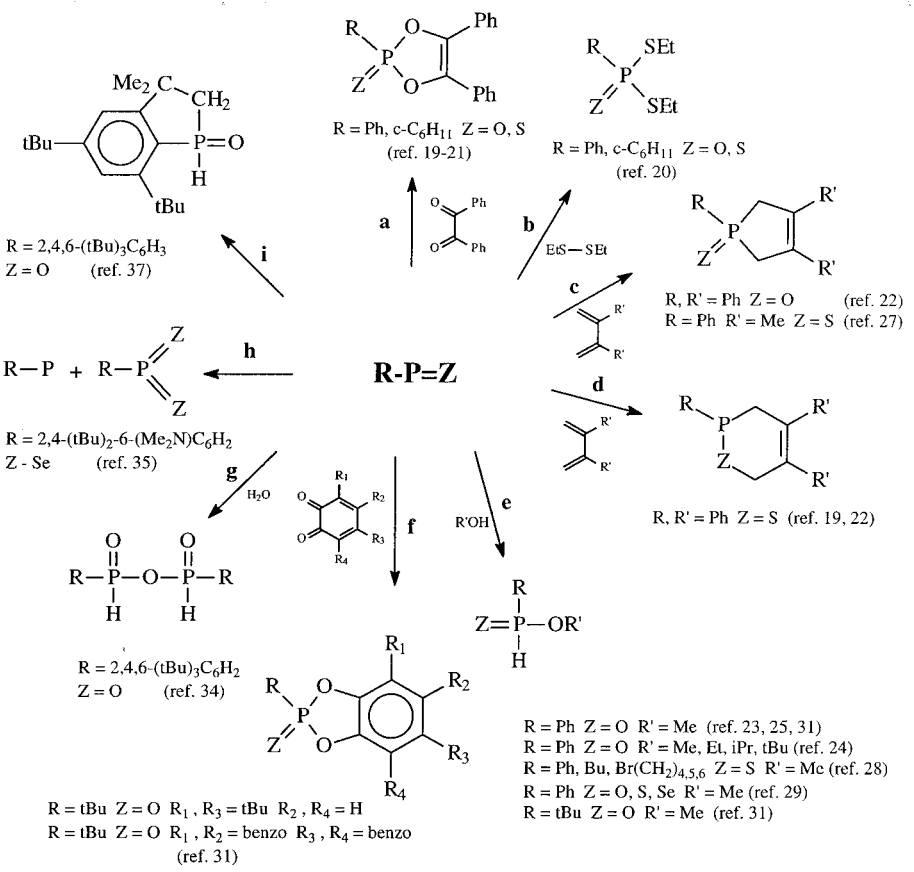

Figure 2. Reactions that have been attributed to phosphinidene chalcogenides R–P=Z.

Carbene-like reactions have long been attributed to phosphinidene chalcogenides, but evidence for their generation has been sparse.[17] Fig. 1 displays eleven reactions that have been proposed, largely on the basis of product studies, to generate R–P=Z. The reactions that have been attributed to R–P=Z are summarized in Fig. 2.

The formation of R–P=O and R–P=S upon the dehalogenation of the corresponding phosphonic or phosphonothioic dichlorides **1** was deduced by Inamoto and his distinguished coworkers in the early 1970s from the products formed by carbene-like additions[18] and insertions from benzil (reaction **a**) and diethyl disulfide (reaction **b**), respectively.[19–21] Formal 1,4-addition to 2,3-diphenylbutadiene was also attributed to Ph–P=O in these experiments (reaction **c**), but a corresponding reaction was not found in experiments in which the intermediacy of Ph–P=S was inferred, and instead 2+4 cycloaddition of the P=S bond was proposed (reaction **d**).[22]

It was again the formation of insertion products from EtSSEt (reaction **b**) and MeOH (reaction **e**) that supported Stille's 1975 suggestion that Ph–P=O was extruded upon pyrolysis of a 7-phosphanorbornadiene oxide **2**.[23] No adducts were obtained when the pyrolysis was carried out in the presence of alkenes or alkynes, and Stille recognized the possibility that addition was occurring to **2** *before* loss of tetraphenylnapthalene.

In 1974 Tomioka had suggested that Ph–P=O is formed by photolysis of a 3-phospholene oxide **3** based on the apparent methanol H–O insertion product (reaction **e**).[24] From a series of elegant fluorescence and quenching experiments Tomioka concluded that this photofragmentation occurred via a singlet excited state.[25] The non-stereospecific fragmentation could be explained by competing disrotatory chelotropic processes forming Ph–P=O, *or* by stepwise fragmentation which would not necessarily lead to free R–P=O.

Product studies suggested the possible generation of phosphinidene chalcogenides from bicyclic and tricyclic molecules in which a strained 3-phospholene chalcogenide unit is present as a substituted 7-phosphanorbornene chalcogenide. Tomioka reported that direct irradiation of 1-phenyl-3-phospholene oxide dimer **4** leads to an apparent H–O insertion product of Ph–P=O (reaction **e**).[26] Mathey found that heating *exo*-dimer **5** to 150°C in the presence of 2,3-dimethylbutadiene led to the apparent 1,4-adduct of Ph–P=S and the diene (reaction c).[27] When the bicyclics **6** were irradiated in the presence of MeOH the products expected from trapping of R–P=S (R=Ph, Bu, $Br(CH_2)_n$; n=4,5,6) by H–O insertion (reaction **e**) were obtained, but Mathey did not suggest phosphinidene sulfide intermediates.[28] Tomioka reported the trapping (via reaction **e**) of the phosphinidene selenide as well as the oxide and sulfide when the phosphole chalcogenide-cyclopentadiene adducts **7** were irradiated in MeOH.[29]

However Quin et al. found that 1-phenyl-3-phospholene oxide **3** (R,R′=H, R″=Me), bicyclic **6** (R=Ph,

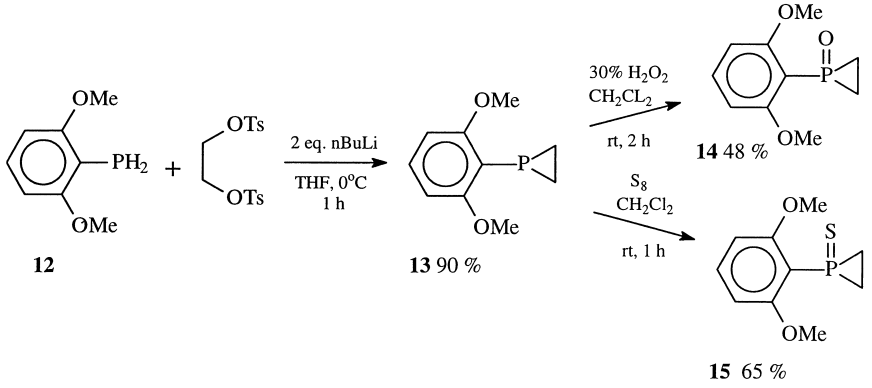

Scheme 5.

Y,Y′=NPh), and its P-sulfide analog did *not* undergo cleavage when irradiated in the absence of MeOH.[30] It was suggested that photo-induced addition of MeOH to 7-phospha-norbornene and 3-phospholene chalcogenides may form five-coordinate intermediates that fragment to the observed products.[30]

In 1978 Quast synthesized the first stable phosphirane oxide **8** by a cyclization that resembles the first step in the Ramberg–Bäcklund reaction.[31,32] Formation of *t*Bu–P=O upon the thermolysis of **8** above 60°C was deduced from the *cis*-di-*tert*-butylethylene coproduct and the formation of products presumed to arise by H–O-insertion (reaction **a**) and formal 1,4-addition to quinones (reaction **f**). In 1982 Quast reported that the disappearance of **8** appeared to be a first-order process whose rate was similar in benzene and dioxane and did not appear to be accelerated by the presence of trapping agents.[33] No adducts were obtained from benzil, biacetyl, 2,3-dimethylbutadiene, or bis(trimethylsilyl)-acetylene.

Quin suggested that the slow decomposition of the bicyclic phosphirane oxide **9** liberated an arylphosphinidene oxide that was trapped by residual water as a phosphinic acid anhydride (reaction **g**).[34]

Recently deselenization of diselenoxo- and selenoxothioxo-phosphoranes **10** yielded the corresponding phosphinidene selenide[35] and sulfide.[36] The selenide Ar–P=Se (Ar=2,4-(tBu)$_2$-6-(Me_2N)C_6H_2) is metastable and its ^{31}P NMR spectrum was recorded; it underwent disproportionation (reaction **h**).[35] The corresponding sulfide Ar–P=S was longer-lived and did not undergo reactions **a** and **b**.[36] Yoshifuji suggested that the N coordinates to the P-atom.

Most recently Cowley reported the pyrolysis of a P(III) oxalate **11** leading to a product that appears to be due to a carbene-like intramolecular C–H insertion by the phosphorus center, reaction **i**.[37]

Against this background, our goal was to simplify the synthesis of phosphirane chalcogenides, and to examine their thermal and photochemical decomposition to determine whether free phosphinidene chalcogenides were formed. If so, the reactivity of free phosphinidene chalcogenides could be explored by carrying out reactions under the conditions that the liberation of the free phosphinidene chalcogenides was verified. Finally, if free phosphinidene chalcogenides are formed by concerted thermolysis of phosphirane chalcogenides, that is by retroaddition reactions, then classical kinetic studies of the thermolysis might allow the elucidation of the retroaddition/addition mechanism and experimentally answer the question whether a non-least motion pathway operates as predicted by the frontier orbital model.

Results

The synthetic sequence in Scheme 5 was followed for the synthesis of the phosphirane oxide **14** and sulfide **15**. 2,6-Dimethoxyphenylphosphirane **13** was prepared from 2,6-dimethoxyphenylphosphine[38] **12** by Li's modification[39] of a procedure devised by Oshikawa and Yamashita.[40] Two-phase oxidations (H_2O_2–CH_2Cl_2 and S_8–CH_2Cl_2) gave the chalcogenides in high yield. The X-ray crystal structures of **13**, **14**, and **15** are presented in Figs. 3–5, respectively. Crystal data and structure refinement parameters are given in Table 1. Selected bond-lengths and angles are given in Table 2.

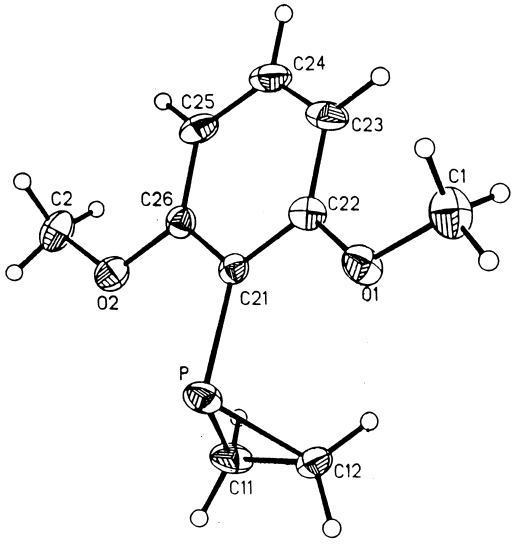

Figure 3. ORTEP drawing of a crystal structure of **13**.

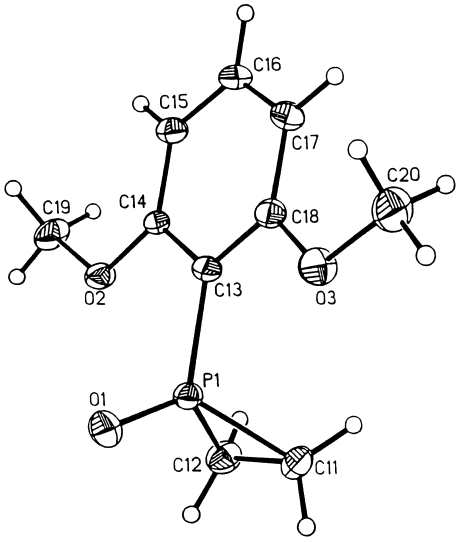

Figure 4. ORTEP drawing of a crystal structure of **14**.

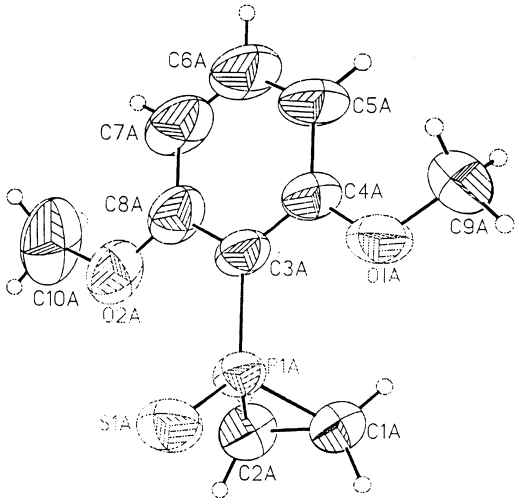

Figure 5. ORTEP drawing of a crystal structure of **15**.

In preliminary thermolysis experiments, heating degassed benzene solutions of **14** and **15** to 80°C in sealed NMR tubes for 3 h led to quantitative yields of ethylene as determined by ^{1}H NMR spectroscopy.

In order to establish the intermediacy of phosphinidene chalcogenides in these reactions, kinetic studies were undertaken of the thermolysis of **14** and **15**. The disappearance of **14** and **15** were clean first-order processes over at least three half-lives in the temperature ranges 44–80 and 44–75°C, respectively.[41] Table 3 compares the first-order rate constants for thermolysis of **14** in benzene with that in acetonitrile, and in benzene with and without EtSSEt (12 vol%, 10× precursor concentration) and CD_3OD (5 vol%, 10× precursor concentration) trapping agents. The rate

Table 1. Crystal data and structure refinement parameters

	13	**14**	**15**
Empirical formula	$C_{10}H_{13}O_2P$	$C_{10}H_{13}O_3P$	$C_{10}H_{13}O_2PS$
Formula weight	196.2	212.2	228.23
Temperature (K)	296	296	298(2)
Crystal system	monoclinic	triclinic	triclinic
Space group	$P2_1/c$	$P\bar{1}$ (bar)	$P\bar{1}$ (bar)
Unit cell dimensions	a=12.578(3) Å	a=8.762(2) Å	a=8.2937(7) Å
	b=5.4450(10) Å	b=11.235(2) Å	b=12.1787(9) Å
	c=15.038(3) Å	c=11.992(2) Å	c=18.6125(11) Å
	β=103.51(3)°	α=76.97(3)°	α=99.353(6)°
		β=75.00(3)°	β=94.314(6)°
		γ=72.80(3)°	γ=108.289(8)°
Volume	1015.9(4) Å^3	1075.1(4) Å^3	1745.2(2)
Z	4	4	6
Density (calculated)	1.283 g/cm^3	1.311 g/cm^3	1.303 g/cm^3
Absorption coefficient	21.24 cm^{-1}	21.21 cm^{-1}	35.64 cm^{-1}
F(000)	416	448	720
Crystal size (mm^3)	0.18×0.28×0.33	0.06×0.44×0.30	0.42×0.33×0.30
θ range for data collection	3.0–113.0°	3.0–113.5°	4.86–123.98°
Index ranges	$0\leq h\leq 13$	$0\leq h\leq 9$	$-9\leq h\leq 9$
	$0\leq k\leq 5$	$-11\leq k\leq 11$	$-14\leq k\leq 14$
	$-16\leq l\leq 15$	$-12\leq l\leq 12$	$0\leq l\leq 22$
Reflections collected	1405	3063	14,643
Independent reflections	1337 (R_{int}=6.50%)	2837 (R_{int}=3.63%)	6000 (R_{int}=4.8%)
Absorption correction	none	none	none
Refinement method	Full-matrix Least-squares	Full-matrix Least-squares	Full-matrix Least-squares
Data-to-parameter ratio	5.3:1	7.0:1	15.3:1
Goodness-of-fit on F^2	1.16	1.05	1.079
Final R indices [$I>2\sigma(I)$]	R=4.56%	R=4.87%	$R1$=7.62%
	wR=5.35%	wR=6.62%	$wR2$=21.75%
R indices (all data)	R=10.72%	R=8.10%	$R1$=9.30%
	wR=6.88%	wR=8.27%	$wR2$=26.63%
Extinction coefficient	–	–	0.0036(7)
Largest diff. peak and hole (e Å^{-3})	0.18 and −0.24	0.29 and −0.32	0.440 and −0.736

Table 2. Selected bond distances (Å) and angles (°) for compounds **13**, **14** and **15**

	13, Z=:	**14**, Z=O[a]	**15**, Z=S[b]
P–Z	–	1.473(4), 1.479(4)	1.9365(15)–1.945(2)
P–C_{ring}	1.820(7), 1.828(7)	1.739(6)–1.759(5)	1.761(4)–1.786(4)
C_{ring}–C_{ring}	1.488(9)	1.552(9), 1.555(8)	1.538(6)–1.558(7)
P–C_{ipso}	1.826(6)	1.792(5), 1.793(6)	1.782(4)–1.791(4)
O–C_{ortho}	1.365(8), 1.365(9)	1.362(7)–1.375(6)	1.351(6)–1.377(5)
O–C_{Me}	1.414(9), 1.417(8)	1.402(9)–1.424(9)	1.417(5)–1.434(5)
Z–P–C_{ipso}	–	116.4(2), 117.4(2)	118.51(13)–119.13(15)
Z–P–C_{ring}	–	123.7(2)–125.0(3)	123.2(2)–124.3(2)
C_{ring}–P–C_{ring}	48.1(3)	52.5(3)–53.0(3)	51.5(2)–53.0(3)
C_{ring}–P–C_{ipso}	101.4(3), 101.5(3)	111.1(3)–111.6(3)	110.1(2)–111.6(2)
O–C_{ortho}–C_{ipso}	114.9(6), 115.7(6)	114.6(5)–115.4(5)	114.1(4)–115.5(4)
C_{Me}–O–C_{ortho}	118.8(5), 119.3(5)	117.6(5)–119.6(5)	118.5(4)–119.7(5)

[a] There are two nearly identical molecules of **14** in the unit cell.
[b] There are three nearly identical molecules of **15** in the unit cell.

Table 3. First-order rate constants for the pyrolysis of **14** and **15**

Precursor	Solvent	Temperature (°C)	Trapping agent	Rate constant (10^{-5} s^{-1})
14	C_6D_6	75.0±0.1	none	7.99±0.15
14	CD_3CN	75.0±0.1	none	12.1±0.4
14	C_6D_6	75.0±0.1	EtSSEt	8.02±0.15
14	C_6D_6	75.0±0.1	CD_3OD	16.4±0.3
15	C_6D_6	65.0±0.1	none	68.3±0.19
15	C_6D_6	65.0±0.1	EtSSEt	69.0±0.17

constant for disappearance of **14** was 50% larger in acetonitrile than in benzene. The presence of EtSSEt did not accelerate the disappearance of **14** or **15**, but the presence of methanol at one molar concentration doubled the rate of disappearance of **14**. The yields of the expected trapping products of the phosphinidene chalcogenide (vide infra) corresponding to **14** in these kinetic experiments were 79±3% (EtSSEt) and 70±2% (CD_3OD) and that corresponding to **15** was 86±1%, as determined by NMR integration.

Fig. 6 displays the Eyring plot for the temperature dependence of the first-order rate constants for the thermolysis of **14** in C_6D_6 and Fig. 7 displays the Arrhenius plot for **15**. The activation parameters derived from these plots are: **14** E_a=32.2±1.3 kcal/mol, log A=16.1±0.8, $\Delta H^{\ddagger}$=31.4±1.3 kcal/mol, $\Delta S^{\ddagger}$=12.9±3.6 eu; **15** E_a=25.8 kcal/mol, log A=13.5±1.1, $\Delta H^{\ddagger}$=25.1±1.6 kcal/mol, $\Delta S^{\ddagger}$=1.1±4.8 eu.

Fig. 8 displays the results of RHF/6-31G* ab initio

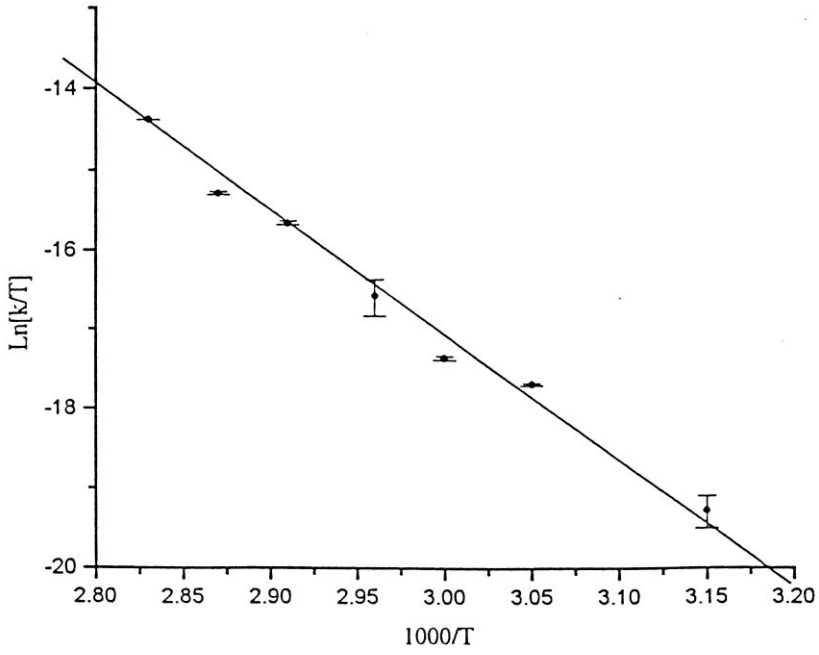

Figure 6. Eyring plot for the pyrolysis of **14** in C_6D_6.

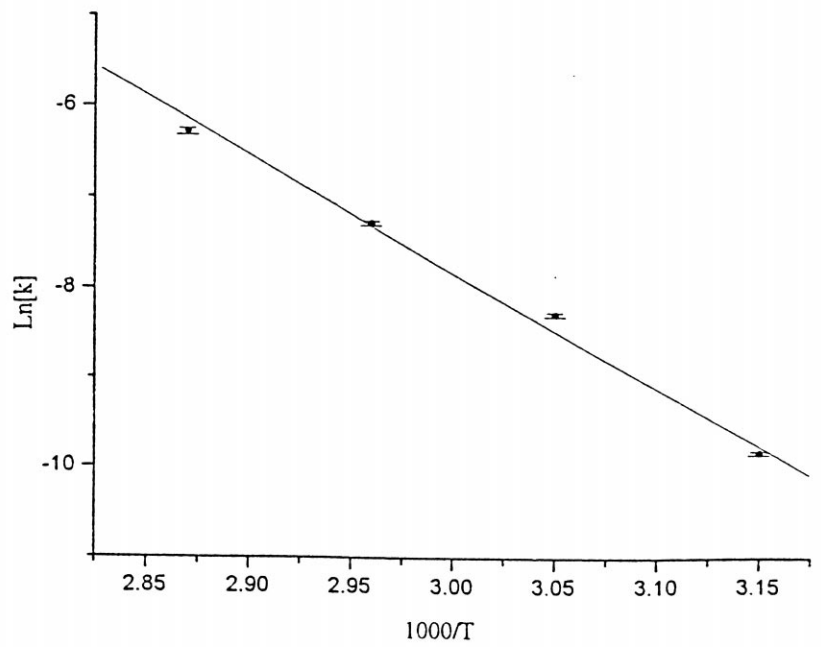

Figure 7. Arrhenius plot for the pyrolysis of **15** in C_6D_6.

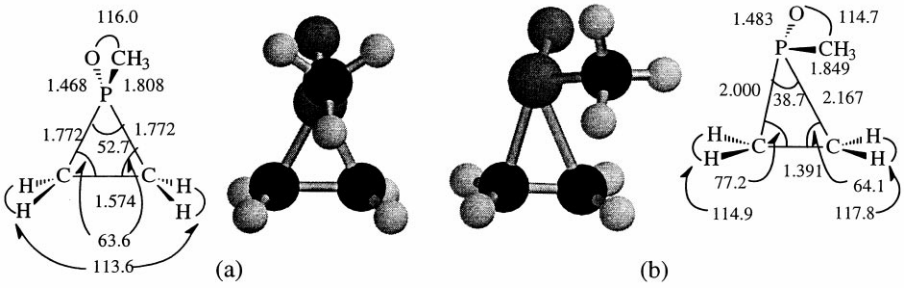

Figure 8. Structures (Å, deg) predicted by SCF 6/31G* calculations for (a) 1-methylphosphirane oxide and (b) the transition state for pyrolysis of (a) to C_2H_4 and Me–P=O.

calculations on a model compound, 1-methylphosphirane oxide and the transition state for its pyrolysis to methylphosphinidene oxide Me–P=O and ethylene.[42] In the transition state (b) the angle between the plane containing the O, P, and C_{Me} atoms and the plane containing the four ring H-atoms is 36°. This angle is 90° in the intact molecule (a).

As indicated in the reactions in Schemes 6 and 7, thermal and photochemical decomposition of **14** and **15** in the presence of various trapping agents gave rise to products that had previously been attributed to phosphinidene chalcogenides. The photolyses were carried out with low-pressure mercury lamps.

S,S-Diethyl 2,6-dimethoxyphenylphosphonodithioate **16** and the corresponding trithioate **18** were purified and gave satisfactory elemental analyses. Their ^{31}P chemical shifts δ ^{31}P=49.1 **16**, 72.4 **18** are similar to those of related

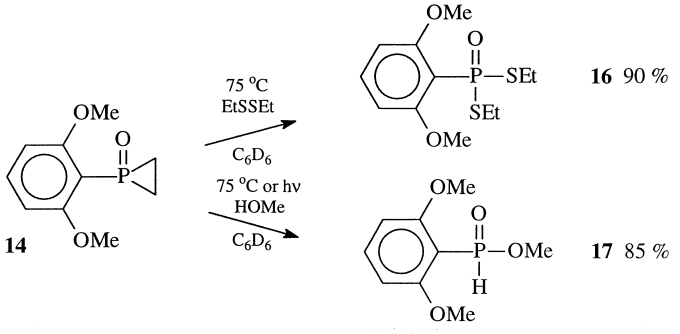

Scheme 6.

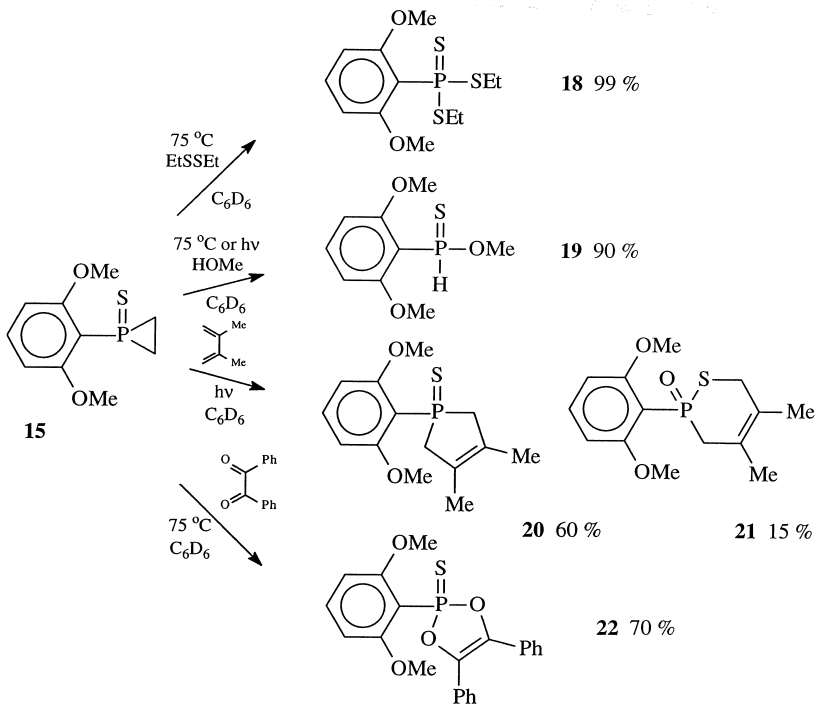

Scheme 7.

compounds: $PhP(O)(SEt)_2$ δ ^{31}P=52.5 ppm,[18] $PhP(S)(SEt)_2$ δ ^{31}P=80.5 ppm.[20] The instability of even purified methyl 2,6-dimethoxyphenylphosphinate **17** and the corresponding *O*-methyl thiophosphinate **19** precluded a satisfactory elemental analysis, but the distinctive phosphinate and thiophosphinate NMR signals made their identification unambiguous: **17** ^{31}P δ=28.3 ppm, J_{P-H}=564 Hz (cf. PhPH(O)OMe ^{31}P δ=29.3 ppm, J_{P-H}=576 Hz),[43] **19** ^{31}P δ=55.9 ppm, J_{P-H}=559 Hz (cf. PhPH(S)OMe ^{31}P δ=69.3 ppm, J_{P-H}=528 Hz).[30]

2,6-Dimethoxyphenyl-3,4-dimethyl-3-phospholene sulfide **20** was identified by comparison with an authentic sample synthesized by condensation of 2,6-dimethoxyphenyllithium with 1-bromo-3,4-dimethyl-3-phospholene[44] followed by treatment with sulfur.

The structure of 3,6-dihydro-4,5-dimethyl-2-(2,6-dimethoxyphenyl)-1-thiophosphorin-2-oxide **21** was deduced from its mass spectrum (M^+=298), its ^{31}P chemical shift ^{31}P δ=60.1 ppm (cf. *t*Bu(Ph)P(O)SMe ^{31}P δ=63.3 ppm),[45] and from Heteronuclear Multiple Bond Correlation (HMBC) and Heteronuclear Multiple Quantum Coherence (HMQC) NMR experiments.[46] (2,6-Dimethoxyphenyl)-3,4-diphenyl-2,5-dioxa-3-phospholene sulfide **22** was identified on the basis of its NMR spectra, ^{31}P δ=96.8 ppm (cf. 1,3,4-triphenyl-2,5-dioxa-3-phospholene sulfide ^{31}P δ=105 ppm).[20] Pure **22** could not be obtained.

Discussion

The improvements in the synthesis of phosphiranes previously reported from this laboratory[14,15,39] and their direct oxidation to phosphirane chalcogenides described here promise ready access to precursors for the thermal and photochemical generation of a range of phosphinidene chalcogenides R–P=Z.

The present kinetic studies indicate clearly that 2,6-dimethoxyphenylphosphinidene oxide and sulfide were generated by pyrolysis of phosphirane oxide **14** and sulfide **15**. The disappearance of **14** and **15** are clean first-order processes whose rates were unchanged in the presence of a high concentration of a trapping agent EtSSEt that led to the formation of 79 and 86%, respectively, of the product expected from insertion of R–P=Z into the S–S bond. These results preclude induced decomposition as a contributor to the disappearance of **14** and **15** and are consistent with a concerted extrusion of R–P=Z. A long-lived reversibly-formed intermediate that can transfer a phosphinidene chalcogenide unit to a substrate is also excluded. A stepwise decomposition to free phosphinidene chalcogenide with a fast second step is rendered unlikely by the activation parameters, the small entropies of activation being consistent with the non-least-motion concerted extrusion depicted earlier but inconsistent with the cleavage of a single P–C bond. There has been little experimental evidence that speaks to the question of whether non-least-motion addition occurs for carbenes and carbene-like species.[47]

The results of ab initio calculations on the dissociation of a model compound 1-methylphosphirane oxide are shown in Fig. 8.[42] A concerted extrusion of Me–P=O is predicted by the calculations, and a non-least-motion transition state is clearly seen. For this model system the calculations predict an entropy of activation of +0.8 eu which compares favorably with the experimental $\Delta S^{\ddagger}$ for **14** and **15** of 12.9±3.6 and 1.1±4.8 eu, respectively. The experimental activation parameters for the presumed non-least-motion extrusion of dimethylsilylene Me_2Si from hexamethylsilirane are $\Delta H^{\ddagger}$=31.6±2.7 kcal/mol, $\Delta S^{\ddagger}$=11.2 eu.[48]

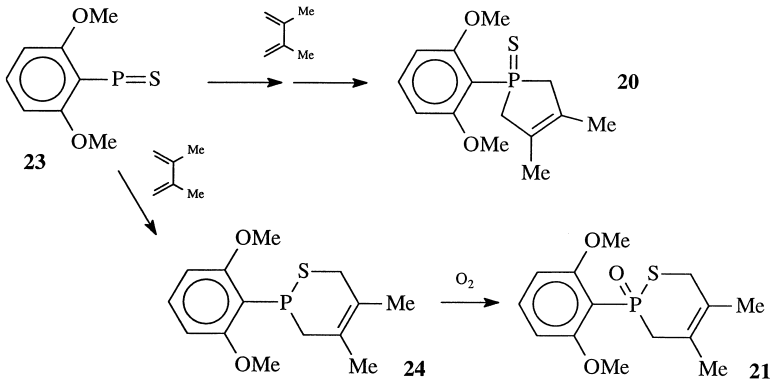

Scheme 8.

The operation of a concerted non-least-motion retroaddition (and addition) pathway that is suggested by the present results supports the applicability of frontier-orbital predictions to reactions with small enthalpic barriers.

That a phosphirane chalcogenide *can* undergo pyrolysis without participation by a trapping agent does not guarantee that it will always do so. The pyrolysis rate for **14** doubled in the presence of CD_3OD, and thus the role of free phosphinide oxide in these reactions remains to be determined by future experiments. The same caution must be exercised regarding the mechanisms of the photolysis of **14** and **15** in the presence of methanol, the photolysis of **15** in the presence of 2,3-dimethylbutadiene and the pyrolysis of **15** in the presence of benzil. The products observed, **17**, **19**–**22**, can be rationalized in terms of reactions previously suggested for phosphinidene chalcogenides (Fig. 2, reactions **a**, **c**–**e**), but kinetic or spectroscopic studies are needed to probe the intermediacy of free phosphinidene chalcogenides in these reactions.

The results reported here do confirm the insertion of phosphinidene chalcogenides into the S–S bond of EtSSEt previously suggested by Inamoto et al. (Fig. 3, reaction **b**).[20] This reaction places the participation of phosphinidene chalcogenides in carbene-like reactions on a firm basis, and their scope will surely be extended.

The formation of both **20** and **21** from photolysis of **15** in the presence of 2,3-dimethylbutadiene is of interest in suggesting that a carbene-like phosphorus center and a P=S π-bond may compete as reaction sites on a phosphinidene sulfide. When $PhP(S)Cl_2$ (**1** R=Ph, Z=S) was dehalogenated with magnesium in the presence of 2,3-dimethyl-1,3-butadiene, the product obtained by Inamoto et al. was attributed to cycloaddition of the P=S π-bond of Ph–P=S.[19,22] That thiophosphorin was converted by air to its oxide.[22] The phospholene sulfide analogous to **20** was *not* found in that experiment,[22] but it was found by Mathey et al. from pyrolysis of **5**.[27] Thus **20** and **21** could arise from competing reactions of a phosphinidene sulfide **23** as shown in Scheme 8.

While the intermediacy of free **23** in the formation of **20** and **21** remains unproved, it may be confidently predicted that the reactions of phosphinidene chalcogenides and their mimics will soon enter the synthetic arsenal of phosphorus chemistry. R–P=Z and the synthetically useful electrophilic two-electron phosphinidene-transition metal complexes developed by the Mathey laboratory[49] are isolobal. When the electrophilicity of phosphinidene chalcogenides is increased, the accessibility of their precursors and the ease of their generation should ensure their widespread use. It is interesting that the reaction with 2,3-dimethylbutadiene suggests that phosphinidene sulfide **23** is more reactive than the corresponding phosphinidene oxide generated from **14**. The corresponding selenide may prove to be even more reactive, and the electrophilicity of R–P=Z can be increased by making R more electron-withdrawing than the 2,6-dimethoxyphenyl group employed here.

Conclusion

Kinetic studies of the pyrolysis of 2,6-dimethoxyphenylphosphirane oxide **14** and sulfide **15** suggest that the corresponding phosphinidene chalcogenide R–P=O and R–P=S are formed by a concerted, non-least-motion extrusion. The pyrolysis rate is not accelerated by the presence of EtSSEt and $RP(Z)(SEt)_2$ products **16** and **18** are formed in high yield, confirming S–S insertion by the free phosphinidene chalcogenides. The kinetic studies provide quantitative evidence for the validity of predictions of frontier-orbital theory for species that undergo reactions with small enthalpic barriers. The products from thermal and photochemical reactions in the presence of other trapping agents are in accord with previously suggested carbene-like reactions of phosphinidene chalcogenides, but a rate acceleration observed for pyrolysis of **14** in the presence of CD_3OD dictates caution in the acceptance of such intermediates without complete mechanistic studies.

Experimental

General data

All preparative reactions were carried out in flame-dried glassware under an atmosphere of dry nitrogen or argon. Photolyses were carried out in a Rayonet RS photochemical reactor (model RPR-208, 120 W radiated power) equipped with low-pressure Hg lamps (254 nm radiation). ^1H, ^{13}C, and ^{31}P NMR spectra were recorded on Varian Unity Plus-300, Gemini-300 (^{13}C 75.4 MHz, ^{31}P 121.4 MHz),

Unity Plus-500 (^{13}C 125 MHz, ^{31}P 202.3 MHz) and Unity-600 (^{13}C 250 MHz) spectrometers. 85% H_3PO_3 was employed as an external ^{31}P standard. Recorded yields are based on starting materials consumed and were determined by integration of ^{31}P spectra. Combined gas chromatography–mass spectrometry was performed on a Hewlett–Packard Model 5890 Series II instrument fitted with a Quadrex 25-m×0.32 mm capillary column coated with 0.5 μm polymethyl(5% phenyl)silicone bonded phase connected to a Model 5971 mass selective detector (quadrupole mass filter), mass spectra recorded above *m*/*e* 40, ionization energy 70 eV.

Materials

Benzene, THF, ether, and pyridine were dried by and distilled from sodium benzophenone ketyl under a nitrogen atmosphere immediately before use. CaH_2 was the drying agent for pentane, cyclohexane, and hexane. CH_2Cl_2 was distilled from P_2O_5. Reagent chemicals were employed as received except as noted: C_6D_6 (Aldrich, 99.6%), *n*-BuLi (Fisher, 1.6 M or Aldrich, 2.5 M in hexane), chloroform-d (Aldrich, 99.8%), CD_2Cl_2 (Aldrich, 99.95%), 1,3-dimethoxybenzene (Aldrich, 99%, distilled under N_2 from Na before use), 2,3-dimethyl-1,3-butadiene (Aldrich, 98%, distilled under N_2 before use), ethylene glycol (Sigma, 99%), H_2O_2 (Aldrich, 30%), $LiAlH_4$ (Aldrich, 95%), CD_3OD (Aldrich, 99.8%), PBr_3 (Aldrich, 97%, distilled under N_2 before use), *p*-toluenesulfonyl chloride (Aldrich, 98%).

2,6-Dimethoxyphenylphosphine was synthesized by the method of Qian et al.[38]

Ethylene glycol ditosylate was synthesized by the method of Corey and Mitra.[50]

2,6-Dimethoxyphenylphosphirane 13. To 2.20 g (5.94 mmol) ethylene glycol ditosylate in a N_2-flushed 250 mL round-bottomed Schlenck flask equipped with a magnetic stirrer bar and a septum were added 150 mL THF and 1.00 g (5.88 mmol) 2,6-dimethoxyphenylphosphine. The flask was cooled to 0°C, and 7.5 mL (12.0 mmol) 1.6 M *n*-BuLi was added dropwise via syringe. The reaction mixture was then stirred for 45 min. A ^{31}P NMR spectrum of an aliquot indicated disappearance of the primary phosphine (^{31}P δ −172) and the appearance of the product (^{31}P δ −254). Excess *n*-BuLi was quenched by addition of 0.1 mL (0.78 mmol) Me_3SiCl. After solvent, excess Me_3SiCl and other volatiles were removed under vacuum, 150 mL pentane was added to precipitate lithium salts. Filtration and concentration under vacuum gave a slightly yellow liquid, 0.98 g (85% crude yield) suitable for oxidation. Pure product was obtained by column chromatography on silica gel with 1:1 CH_2Cl_2-hexane eluent followed by recrystallization from 1:9 CH_2Cl_2-hexane at −20 °C. **13**: mp 89.5–90.5°C ^{31}P NMR (202.6 MHz, CD_2Cl_2) δ −253.7; ^{1}H NMR (500 MHz, CD_2Cl_2) δ 1.13–1.17 (m, 4H, CH_2), 3.84 (s, 6H, CH_3), 6.47 (dd, 2H J_{P-H}=2.0 Hz, J_{H-H}=8.0 Hz, *m-H*), 7.02 (t, 1H, J_{P-H}=8.1 Hz, *p-H*); ^{13}C{^{1}H} NMR (125.7 MHz, CD_2Cl_2) δ 10.0 (d, J_{P-C}=40.2 Hz, *C*H_2), 56.1 (s, *C*H_3), 103.8 (s, *m-C*), 116.8 (d, J_{P-C}=45.1 Hz, *ipso-C*), 130.0 (s, *p-C*), 163.6 (d, J_{P-C}=5.9 Hz, *o-C*); elemental analysis, calcd for $C_{10}H^{13}O_2P$ C 61.22%, H 6.68%; obsvd C 60.98%, H 6.85%.

2,6-Dimethoxyphenylphosphirane oxide 14. To 0.99 g (5.00 mmol) **13** dissolved in 30 mL CH_2Cl_2 in a 100 mL flask equipped with a magnetic stirrer bar was added 2.8 mL (25.0 mmol) 30% H_2O_2. After 48 min of stirring a ^{31}P NMR spectrum of an aliquot indicated that **13** was consumed and **14** was formed. The reaction mixture was extracted with water (3×20 mL) and brine (3×20 mL). The colorless organic phase was dried with Na_2SO_4, filtered, and volatiles removed under vacuum, leaving 1.01 g (95% crude yield) light-yellow oily product. This was purified by chromatography on silica gel with 10:10:2 CH_2Cl_2–EtOAc–EtOH eluent, yielding **14** as a white solid (0.51 g, 48%) that was recrystallized from EtOAc: ^{31}P NMR (121.4 MHz, CD_2Cl_2) δ −50.3; ^{1}H NMR (500 MHz, CD_2Cl_2) δ 1.16–1.25 (m, 2H, H_{syn}), 1.92–2.03 (m, 2H, H_{anti}), 3.90 (s, 6H, CH_3), 6.63 (dd, 2H, J_{P-H}=5.7 Hz, J_{H-H}=8.7 Hz, *m-H*), 7.48 (t, 1H, J_{H-H}=8.7 Hz, *p-H*); ^{13}C{^{1}H} (150.9 MHz, CD_2Cl_2) δ 9.9 (d, J_{P-C}=26.0 Hz, CH_2), 56.5 (s, CH_3), 104.1 (d, J_{P-C}=4.5 Hz, *m-C*), 108.4 (d, J_{P-C}=122.1 Hz, *ipso-C*), 135.5 (s, *p-C*), 162.2 (s, *o-C*); elemental analysis, calcd for $C_{10}H_{13}O_3P$ C 56.59%, H 6.18%; obsvd C 56.44%, H 6.23%.

2,6-Dimethoxyphenylphosphirane sulfide 15. To 0.99 g (5.00 mmol) **13** dissolved in 30 mL CH_2Cl_2 in a 100 mL flask equipped with a magnetic stirrer bar was added 1.00 g (31 mmol) sublimed sulfur. After 45 min of stirring a ^{31}P NMR spectrum of an aliquot indicated the disappearance of **13** and the formation of **15**. Solvent was removed under vacuum and the residue mixed with 5 mL CH_2Cl_2 and filtered to remove excess sulfur. Evaporation of solvent left 1.12 g (98% crude yield) yellow oil that was purified by chromatography on silica gel with CH_2Cl_2 eluent, yielding 0.75 g (65%) **15** as a yellow solid. X-Ray quality crystals were obtained by recrystallization from 1:4 EtOAc–hexane. **15**: ^{31}P NMR (121.4 MHz, CD_2Cl_2) δ −90.7; ^{1}H NMR (300 MHz, CD_2Cl_2) δ 1.47–1.57 (m, 2H, H_{syn}), 1.72–1.82 (m, 2H, H_{anti}), 3.92 (s, 6H, CH_3) 6.60 (dd, 2H, J_{P-H}=5.7 Hz, J_{H-H}=8.4 Hz, *m-H*), 7.48 (t, J_{H-H}=8.4 Hz, *p-H*); ^{13}C{^{1}H} NMR (150.9 MHz, CD_2Cl_2) δ 13.5 (d, J_{P-C}= 11.5 Hz, *C*H_2), 56.7 (s, *C*H_3), 104.3 (d, J_{P-C}=6.2 Hz, *m-C*), 109.3 (d, J_{P-C}=97.6 Hz, *ipso-C*), 134.9 (s, *p-C*), 161.8 (s, *o-C*); elemental analysis, calcd for $C_{10}H_{13}O_2PS$ C 52.62%, H 5.75%; obsvd C 52.55%, H 5.99%.

1-Bromo-3,4-dimethyl-3-phospholene was synthesized by the method of Gruneich and Wisian–Neilson.[44]

1-(2,6-Dimethoxyphenyl)-3,4-dimethyl-3-phospholene sulfide 20. A 100-mL three-necked flask equipped with a pressure-equalizing dropping funnel, a magnetic stirring bar, and an N_2-inlet was charged with 3.165 g (22.9 mmol) 1,3-dimethoxybenzene and 50 mL THF. The reaction mixture was cooled to 0°C, and 9.15 mL (22.9 mmol) 2.5 M *n*-BuLi was added dropwise. The reaction mixture was than allowed to warm to room temperature and stirred for 4 h. To this yellowish turbid solution, cooled to −78°C, 3.00 g (15.5 mmoles) 1-bromo-3,4-dimethyl-3-phospholene in 25 mL THF was added slowly, and the reaction mixture was allowed to warm to room temperature.

The reaction mixture turned from yellow to orange and then to brown in 2 h. A ^{31}P NMR spectrum of an aliquot revealed a strong new peak at ^{31}P δ −33 (Cf. 1-mesityl-3-phospholene ^{31}P δ −31).[14] Solvent was removed under vacuum, and 80 mL pentane was added to precipitate salts. The reaction mixture was stirred 10 min., filtered, and the pentane removed under vacuum. The orange residue was crude 1-(2,6-dimethoxyphenyl)-3,4-dimethylphospholene which was dissolved in 40 mL CH_2Cl_2 and filtered through a small pad of silica gel. 1.5 g (46.9 mmol) S_8 was added to this solution, which was then stirred for 1 h. The ^{31}P δ −33 signal had been replaced by one at ^{31}P δ 41. Volatiles were removed under vacuum, another 4 mL CH_2Cl_2 was added, and residual sulfur was removed by filtration. Volatiles were removed at 90°C/1 torr, and the 2.7 g residue was chromatographed on silica gel with CH_2Cl_2 eluent, giving a white solid that was recrystallized from 1:9 CH_2Cl_2–hexane at −20°C, yielding 2.3 g (53% based on 1-bromo-3,4-dimethyl-3-phospholene) pure **20**: mp 187.5–188.5°C; ^{31}P NMR (121.4 MHz, CD_2Cl_2) δ 41.4; ^{1}H NMR (300 MHz, CD_2Cl_2) δ 1.77 (s, 6H=CC*H*$_3$), 2.85 (bt, 2H J=16.5 Hz, C*H*H *syn* to S), 3.41(dm, 2H, J=17.2 Hz, CH*H*, *anti* to S), 3.89 (s, 6H, C*H*$_3$), 6.08 (dd, 2H, J_{P-H}=4.2 Hz, J_{H-H}=8.4 Hz, *m-H*), 7.40 (t, 1H, J_{H-H}=8.4 Hz, *p-H*); $^{13}C\{^{1}H\}$ NMR (125.9 MHz, CD_2Cl_2) δ 16.4 (d, J_{P-C}=13 Hz, =C*C*H$_3$), 47.7 (d, J_{P-C}=58 Hz, *C*H$_2$), 56.3 (s, O*C*H$_3$), 104.7 (d, J_{P-C}=6 Hz, *m-C*), 111.8 (d, J_{P-C}=74 Hz, *ipso-C*), 127.4 (d, J_{P-C}=9 Hz, *C*=*C*), 133.8 (s, *p-C*), 160.9 (s, *o-C*); elemental analysis, calcd for $C_{14}H_{19}O_2PS$ C 59.56%, H 6.78%; obsvd C 59.41%, H 6.92.

Single crystal X-ray analysis of 13, 14, and 15

The data were collected using a Siemens R3m/V diffractometer (**13**, **14**)with a graphite monochrometer and a Bruker SMART Charge Coupled Device (CCD) Detector System X-Ray Diffractometer (**15**), using Cu Kα radiation (λ=1.54178 Å). The structures were solved by direct methods. Structure solution and refinement were carried out employing SHELXTL PLUS. The hydrogen atoms were treated using the appropriate Riding model. Projection views of **13**, **14**, and **15** are shown in Figs. 3–5, respectively with non-hydrogen atoms represented by 25% probability ellipsoids.

Kinetic studies of the pyrolysis of 14 and 15

A sealed capillary tube containing a C_6D_6 solution of MeP(O)(OMe) used as an 'external' standard for ^{31}P NMR integrations was placed in a 4 mm o.d.×150 mm pyrex tube. The reaction mixtures were 0.1 M solutions of **14** or **15** (5.000 mg, 0.02356 mmol, **14** in C_6D_6 or CD_3CN, 5.000 mg, 0.02191 mmol, **15** in C_6D_6) to which trapping agents, when employed, were added (0.030 mL, 0.022 mmol, EtSSEt; 0.010 mL, 0.24 mmol, CD_3OD). The reaction mixtures were degassed at 10^{-5} torr via a freeze-pump–thaw three-cycle process, and then the tubes were sealed with a torch. The samples were thermostatted at various temperatures by immersion in the vapors of azeotropic mixtures whose boiling points are given below.

T	Azeotrope
79.9±0.1 °C	*i*PrOH:H_2O=88:12
75.0±0.1 °C	CH_3CN:EtOAc=23:77
70.0±0.1 °C	cyclohexane:H_2O=92:8
65.0±0.1 °C	CH_3CN:CCl_4=17:83
60.0±0.1 °C	CHC_{l3}:hexane=72:28
55.0±0.1 °C	$ClCH_2CH_2Cl$:EtOH=86:14
44.0±0.1 °C	CS_2:*i*PrOH=72:28

The temperature of each vapor bath was measured over a week with a 0.01°C precision thermometer, and the variation was less than 0.1°C. ^{31}P NMR spectra were recorded at evenly spaced intervals (the reaction mixtures were quenched in cold water), and the concentrations of the phosphirane chalcogenide (and of the product of reaction with trapping agent when present) were determined by comparison of integrated peak areas with those of the 'external' standard. In each kinetic run three measurements were taken at each time interval, which was measured with a stop-watch. The plots of $\ln[C_o/C]$ versus time were linear in each case, and first-order rate constants and their uncertainties were calculated from the slopes of the linear-least squares fitted lines and their standard deviations. Rate constants for pyrolysis of **14** at 75°C in C_6D_6 and in CD_3CN with no added trapping agent and in C_6D_6 in the presence of EtSSEt and CD_3OD and for pyrolysis of **15** at 65°C in C_6D_6 without and with added EtSSEt are displayed in Table 3.

Rate constants for the disappearance of **14** in C_6D_6 without trapping agent were determined at all seven temperatures, while for **15** in C_6D_6 without trapping agent rate measurements were made at 44, 55, 65, and 75°C. Plots of ln k and ln k/T versus 1/T were linear. From these Arrhenius and Eyring plots the activation parameters and their uncertainties included in the discussion section were computed from the slopes and intercepts of the linear least-squares fitted lines and their standard deviations. The Eyring plot for **14** is shown in Fig. 6 and the Arrhenius plot for **15** in Fig. 7. The original data including all the first-order kinetic plots may be consulted.[51]

Thermal and photochemical trapping experiments

Pyrolysis of 14 in the presence of EtSSEt. 50 mg (0.24 mmol) **14** and 0.30 mL (2.4 mmol) EtSSEt were dissolved in 2.1 mL C_6D_6 producing a solution 0.1 M in **14** and 1.0 M in EtSSEt. This mixture in a Pyrex tube was degassed to 10^{-5} torr via three freeze-pump–thaw cycles, and the tube was sealed with a torch and heated at 75°C for 3 h. ^{31}P NMR spectroscopy indicated 95% conversion of **14** and a 90% yield of **16**. Volatiles were removed from the slightly yellow reaction mixture by heating at 60°C/1 torr. The residue was chromatographed on silica gel with 1:50 EtOH–CH_2Cl_2 eluent yielding 22 mg (30%) pure **16** as colorless liquid: ^{31}P NMR (121.4 MHz, $CDCl_3$) δ 49.5; ^{1}H NMR (300 MHz, $CDCl_3$) δ 1.23 (t, 6H, J_{H-H}=7.2 Hz, SCH_2CH_3), 2.80–3.00 (m, 4H, SCH_2), 3.76 (s, 6H OCH_3), 6.46 (dd, 2H, J_{P-H}=5.7 Hz, J_{H-H}=8.4 Hz, *m-H*), 7.53 (t, 1H, J_{H-H}=8.4 Hz, *p-H*); $^{13}C\{^{1}H\}$ NMR (125.7 MHz, $CDCl_3$) δ 16.1 (s, SCH_2CH_3), 25.0 (s, S_CH_2), 56.1 (s, OCH_3), 104.7 (s,

m-C), 112.0 (d, J_{P-C}=103.9 Hz, *ipso-C*), 134.5 (s, *p-C*), 162.0 (s, *o-C*); MS (EI) *m/e* (relative intensity) 306 (M^+, 5), 277 (28), 245 (100), 217 (39), 199 (33), 187 (15), 185 (57), 170 (13), 169 (10), 155 (30), 141 (10), 139 (13), 138 (11), 123 (13), 109 (13), 107 (19), 95 (15), 92 (13), 79 (12), 77 (21), 76 (15), 64 (15), 47 (10); elemental analysis, calcd for $C_{12}H_{19}O_3PS_2$ C 47.04%, H 6.25%; obsvd C 46.72%, H 6.52%.

Pyrolysis of 14 in the presence of MeOH. 50 mg (0.24 mmol) **14** and 0.50 mL (12.3 mmol) MeOH were dissolved in 1.9 mL CD_2Cl_2 to produce a solution 0.1 M in **14** and 5 M in MeOH. This mixture was placed in a Pyrex tube, degassed and sealed as above, and heated at 75°C for 3 h. ^{31}P NMR spectroscopy indicated 99% conversion and an 85% yield of **17**. Volatiles were removed from the slightly yellow reaction mixture by heating at 75°C/l torr; yielding 31.5 mg (61%) **17** as a white solid that decomposes above 80°C and slowly at room temperature. A satisfactory elemental analysis was not obtained. **17**: ^{31}P NMR (121.4 MHz, $CDCl_3$) δ 28.3 (d, J_{H-P}=564 Hz); ^{1}H NMR (300 MHz, $CDCl_3$) δ 3.87 (s, 3H, POCH_3), 3.90 (s, 6H, COCH_3), 6.56 (dd, 2H, J_{H-H}=8.4 Hz, *m-H*), 7.41 (t, 1H, J_{H-H}=8.4 Hz, *p-H*), 8.62 (d, 1H, J_{P-H}=564 Hz, PH); ^{13}C{^{1}H} NMR (75.4 MHz, $CDCl_3$) δ 54.5 (s, POCH_3), 56.0 (s, COCH_3), 105.5 (d, J_{P-C}=8.4 Hz, *m-C*), 112.7 (d, J_{P-C}=104 Hz, *ipso-C*), 133.9 (s, *p-C*), 161.1 (s, *o-C*); MS (El) *m/e* (relative intensity) 217 (21), 216 (M, 100), 197 (46), 185 (16), 184 (14), 183 (63), 138 (39), 137 (34), 121 (19), 109 (40), 107 (19), 79 (33), 78 (15), 77 (33), 76 (15), 65 (14), 64 (10), 63 (16), 51 (13), 47 (21).

Photolysis of 14 in the presence of MeOH. 50 mg (0.24 mmol) **14** and 0.50 mL (12.3 mmol) MeOH were dissolved in 1.9 ml CD_2Cl_2 to produce a solution 0.1 M in **14** and 5 M in MeOH. The mixture was placed in a quartz tube, degassed and sealed as above, and irradiated at 254 nm for 100 min. ^{31}P NMR spectroscopy indicated 99% conversion of **14** and an 80% yield of **17**. Volatiles were removed by heating at 75°C/1 torr leaving 25.1 mg (48%) **17** as a white solid whose ^{31}P, ^{1}H, and ^{13}C NMR spectra were identical with those obtained in the thermolysis experiment reported above.

Pyrolysis of 15 in the presence of EtSSEt. 55 mg (0.24 mmol) **15** and 0.30 mL (2.4 mmol) EtSSEt were dissolved in 2.1 mL C_6D_6 producing a solution 0.1 M in **15** and 1.0 M in EtSSEt that was placed in a Pyrex tube and degassed and sealed as above. After the reaction mixture was heated at 65°C for 3 h, ^{31}P NMR spectroscopy indicated 99% conversion of **15** and a 96% yield of **18**. Volatiles were removed from the slightly yellow reaction mixture by heating at 60°C/l torr. The residue was chromatographed on silica gel with 1:50 EtOH–CH_2Cl_2 eluent yielding 32 mg (41%) pure **18** as a light yellow liquid: ^{31}P NMR (121.4 MHz, $CDCl_3$) δ 72.4; ^{1}H NMR (300 MHz, $CDCl_3$) δ 1.37 (t, 6H, J_{H-H}=6.6 Hz, SCH_2CH_3), 2.98–3.12 (m, 4H, SCH_2) 3.84 (s, 6H, OCH_3), 6.61 (dd, 2H, J_{P-H}=5.9 Hz, J_{H-H}=8.4 Hz, *m-H*), 7.40 (t, 1H, J_{H-H}=8.4 Hz, *p-H*), ^{13}C{^{1}H} NMR (75.4 MHz, $CDCl_3$) δ 15.1 (d, J_{P-C}=7.1 Hz, SCH_2CH_3), 28.1 (s, SCH_2), 56.0 (s, COCH_3), 105.2 (d, J_{P-C}=7 Hz, *m-C*), 113.8 (d, J_{P-C}=97.4 Hz, *ipso-C*), 133.9 (s, *p-C*), 161.1 (s, *o-C*); MS (EI) *m/e* (relative intensity) 322 (M, 14), 294 (14), 262 (52), 261 (32), 229 (30), 201 (16), 200 (42), 185 (52), 170 (32), 169 (25), 167 (17), 153 (10), 151 (12), 139 (19) 138 (100), 123 (18), 109 (18), 108 (10), 107 (14), 95 (19), 77 (12), 63 (33); elemental analysis, calcd for $C_{12}H_{19}O_2PS_2$ C 44.70%, H 5.94%; obsvd C 44.61%, H 6.32%.

Pyrolysis of 15 in the presence of MeOH. 55 mg (0.24 mmol) **15** and 0.50 mL (12.3 mmol) MeOH were dissolved in 1.9 mL CD_2Cl_2 to produce a solution 0.1 M in **15** and 5 M in MeOH. This mixture was placed in a Pyrex tube, degassed, and sealed as above, and heated at 65°C for 3 h. ^{31}P NMR spectroscopy indicated 99% conversion of **15** and a 90% yield of **19**. Volatiles were removed from the light yellow reaction mixture by heating at 69°C/l torr, yielding 36.7 mg (66%) **19** as a light yellow solid that decomposes above 75°C and slowly at room temperature. A satisfactory elemental analysis was not obtained. **19**: ^{31}P NMR (121.4 MHz, $CDCl_3$) δ 51.9 (d, J_{H-P}=559 Hz); ^{1}H NMR (300 MHz, $CDCl_3$) δ 3.80 (s, 3H, POCH_3), 3.86 (s, 6H, COCH_3), 6.54 (dd, 2H, J_{H-H}=8.4 Hz, *m-H*), 7.37 (t, 1H, J_{H-H}=8.4 Hz, *p-H*). 8.58 (d, 1H, J_{P-H}= 559 Hz, PH); ^{13}C {^{1}H} NMR (75.4 MHz, $CDCl_3$) δ 52.6 (s, POCH_3), 56.4 (s, COCH_3), 105.4 (d, J_{P-C}=5.6 Hz, *m-C*), 111.7 (d, J_{P-C}=94 Hz, *ipso-C*), 133.7 (s, *p-C*), 161.0 (s, *o-C*); MS (EI) *m/e* (relative intensity) 232 (M, 85), 200 (61), 199 (51), 185 (100), 169 (35), 168 (11), 167 (45), 155 (11), 153 (26), 139 (21), 138 (10), 137 (13), 109 (14), 107 (11), 95 (11), 93 (23), 91 (11), 77 (11), 63 (26), 47 (10).

Photolysis of 15 in the presence of 2,3-dimethyl-1,3-butadiene. 55 mg (0.24 mmol) **15** and 0.27 mL (2.4 mmol) 2,3-dimethyl-1,3-butadiene were dissolved in 2.13 mL CD_2Cl_2 producing a solution 0.1 M in **15** and 1 M in diene. This mixture was placed in a quartz tube, degassed and sealed as above, and irradiated at 15°C with 254 nm radiation for 100 min. A ^{31}P NMR spectrum indicated 99% conversion of **15** and a 60% yield of **20** together with a 15% yield of a second product **21**. Volatiles were removed under vacuum from the light yellow reaction mixture, and the residue was chromatographed on silica gel with CH_2Cl_2 eluent to give two fractions. The second consisted of 40.6 mg (60%) **20**, identical in its ^{31}P, ^{1}H, and ^{13}C NMR spectra with those reported above for an authentic sample. The first fraction consisted of 10.7 mg (15%) **21** that could not be brought to analytical purity: ^{31}P NMR (121.4 MHz, CD_2Cl_2) δ 60.1; ^{1}H NMR (500 MHz, CD_2Cl_2) δ 1.87 (d, 3H, J_{P-H}=5.2 Hz, PCH_2CCH_3), 1.92 (s, 3H, SCH_2CCH_3), 3.17–3.57 (m, 4H, SCH_2 and PCH_2), 3.90 (s, 6H, OCH_3), 6.62 (dd, J_{P-H}= 5.0 Hz, J_{H-H}=8.4 Hz, *m-H*), 7.38 (t, 1H, J_{H-H}=8.7 Hz, *p-H*); ^{13}C{^{1}H} NMR (125.9 MHz, CD_2Cl_2) δ 19.2 (s, PCH_2CCH_3), 21.5 (s, SCH_2CCH_3), 34.5 (d, J_{P-C}=7.8 Hz, SCH_2), 45.0 (d, J_{P-C}=43.1 Hz, PCH_2), 56.3 (s, OCH_3), 105.1 (d, J_{P-C}=7.8 Hz, *m-C*), 114.7 (d, J_{P-C}=84 Hz, *ipso-C*), 126.5 (s, SCH_2), 132.0 (d, J_{P-C}=15.7 Hz, PCH_2), 133.6 (s, *p-C*), 159.9 (s, *o-C*); The ^{1}H–^{13}C correlations observed in HMQC and HMBC 2-D NMR experiments are listed in Table 4. MS (EI) *m/e* (relative intensity) 298 (M, 1), 283 (14), 282 (84), 267 (13), 250 (13), 249 (75), 186 (10), 185 (100), 170 (28), 167 (25), 139 (14), 138 (16), 123 (18), 113 (13), 111 (24), 109 (20), 107 (21), 97 (10), 95 (23), 91 (13), 83 (13), 79 (14), 77 (23), 53 (15), 51 (11), 41 (25).

Table 4. Hydrogen–carbon correlations observed in 2-D-NMR experiments on **21**

	HMQC correlation (one-bond)	HMBC correlations (multiple-bond)
^{1}H δ	^{13}C δ	^{13}C δ
1.87 (3H)	19.2	34.5, 126.5, 132.0
1.93 (3H)	21.5	45.0, 126.5, 132.0
3.21 (1H)	34.5	19.2, 126.5, 132.0
3.31 (1H)	34.5	21.5, 126.5, 132.0
3.31 (1H)	45.0	21.5, 126.5, 132.0
3.54 (1H)	45.0	21.5, 126.5, 132.0
3.90 (6H)	56.3	159.9
6.62 (2H)	105.1	105.1, 114.7
7.38 (1H)	133.6	105.1, 114.7, 159.9

Pyrolysis of 15 in the presence of benzil. 55 mg (0.24 mmol) **15** and 0.5 mL (2.4 mmol) benzil were dissolved in 2.4 mL C_6D_6 producing a solution 0.1 M in **15** and 1 M in benzil. This mixture was placed in a Pyrex tube, degassed, and sealed as above, and heated at 65°C for 3 h. A ^{31}P NMR spectrum indicated 99% conversion of **15** and a 70% yield of **22**. Volatiles were removed from the yellow reaction mixture under vacuum. The residue was chromatographed on silica gel with CH_2Cl_2 eluent, yielding 20 mg (20%) **22** as a light yellow solid with a broad melting point, 198–220°C that did not give a satisfactory elemental analysis. **22**: ^{31}P NMR (121.4 MHz, $CDCl_3$) δ 96.8; ^{1}H NMR (300 MHz, $CDCl_3$) δ 3.83 (s, 6H, C*H*$_3$), 6.25 (d, 2H, J_{H-H}=8.4 Hz, Ar-*m-H*), 6.79–6.89 (m, 4H), 6.92–7.05 (m, 4H), 7.87–7.91 (m, 4H); $^{13}C\{^{1}H\}$ NMR (75.4 MHz, $CDCl_3$) δ 56.5 (s, O*C*H$_3$), 104.6 (d, J_{P-C}=12 Hz, Ar-*m-C*), 117.5 (d, J_{P-C}=88 Hz, Ar-*ipso-C*), 125.3 (s, O–*C*=), 129.0 (s, Ph-*o*- or *m*-*C*), 130.0 (s, Ph-*o*- or *m*-*C*), 130.2 (s, Ph-*ipso*-*C*), 133.7 (s, Ar-*p*-*C*), 134.5 (s, Ph-*p*-*C*), 161.6 (d, J_{P-C}= 5 Hz, Ar *o*-*C*).

Acknowledgements

This work has received financial support from National Science Foundation Grant CHE-9632897. NMR instrumentation was made available in part through NIH Shared Instrument Grants RR-02004, RR-05018 and RR-07155. Dr Frank Borkenhagen provided valuable experimental advice.

References

1. Gaspar, P. P.; Li, X.; Silverman, J.; Haile, T; Pae, D. H.; Xiao, M. Frontier orbital control of silylene addition to olefins. *Progress in Organosilicon Chemistry*; Marcineac, B., Chojnowski, J. Eds.; Gordon and Breach: Basel, 1995, pp 247–262.

2. A referee has kindly pointed out that a strong perturbation, such as that provided by a co-reactant, is required to localize a lone pair in one 3p AO of a closed-shell singlet phosphinidene. For a proper representation of the valence orbital occupation in the $^{3}\Sigma^{-}$, $^{1}\Delta$, and $^{3}\Sigma^{+}$ states of PH., see: Frison, G.; Mathey, F.; Sevin, A. J. *Organomet. Chem.* **1998**, *570*, 225–234.

3. Skell, P. S.; Woodworth, R. C. *J. Am. Chem. Soc.* **1956**, *78*, 4496–4497.

4. Gaspar, P. P.; Hammond, G. S. The spin states of carbenes. In *Carbene Chemistry*; Kirmse, W., Ed; 1st ed.; Academic: New York, 1964; pp235–274; Spin states in carbene chemistry. In *Carbenes* Vol. II, Moss, R. A., Jones, M. Jr., Eds.; Wiley: New York, 1975; pp 207–362.

5. Gaspar, P. P.; Beatty, A. M.; Chen, T.; Haile, T.; Lei, D.; Winchester, W. R.; Braddock-Wilking, J.; Rath, N. P.; Klooster, W.T.; Koetzle, T. F.; Mason, S. A.; Albinati, A. *Organometallics*. **1999**, *18*, 3921–3932.

6. Moore, W. R.; Moser, W. R.; Laprade, J. E. *J. Org. Chem.* **1963**, *28*, 2200–2205; see also: Jerosch Herold, B.; Gaspar, P. P. *Fortschr. Chem. Forssch*. **1965**, *5*, 89–146.

7. Hoffmann, R. *J. Am. Chem. Soc.* **1968**, *90*, 1475–1485.

8. Keating, A. E.; Garcia-Garibay, M. A.; Houk, K. N. *J. Am. Chem. Soc.* **1997**, *119*, 10805–10809 and earlier references contained therein.

9. Anwari, F.; Gordon, M. S. *Isr. J. Chem.* **1983**, *23*, 129–132.

10. Fleming, I. *Frontier Orbitals and Organic Chemical Reactions*, Wiley: London, 1976.

11. Jasinski, J. M.; Becerra, R.; Walsh, R. *Chem. Rev.* **1995**, *95*, 1203–1228.

12. Houk, K. N.; Rondan, N. G.; Mareda, J. *Tetrahedron* **1985**, *41*, 1555–1563.

13. Lei, D.; Gaspar, P. P. *Organometallics* **1985**, *4*, 1471–1473.

14. Li, X.; Lei, D.; Chiang, M. Y.; Gaspar, P. P. *J. Am. Chem. Soc.* **1992**, *114*, 8526–8530; *Phosphorus, Sulfur Silicon Relat. Elem.* **1993**, *76*, 71.

15. Li, X. *Stereospecific Synthesis of Phosphiranes and Mechanisms of Phosphinidene Reactions*; Washington University: St. Louis, May 1994.

16. That phosphinidene chalcogenides are isolobal with singlet carbenes was first pointed out by Schoeller and Niecke in a seminal communication: Schoeller, W. W.; Niecke, E. *J. Chem. Soc., Chem. Commun.* **1982**, 569–570.

17. For a review of work up to 1990, see: Quin, L. D.; Szewczyk, J. Oxo-, thioxo-, and selenoxophosphines. In *Multiple bonds and low coordination in phosphorus chemistry*, Regitz, M., Scherer, O. J., Eds. Georg Thieme: Stuttgart, 1990; pp 352–366.

18. 1,4-Addition to dienes is not commonly observed for carbenes themselves, but silylenes and germylenes have been shown to undergo their frequently found formal 1,4-additions via 1,2-addition followed by a vinylheterocyclopropane to heterocyclopentene rearrangement See: Lei, D.; Gaspar, P. P. *J. Chem. Soc., Chem. Commun.* **1985**, 1149–1151; Bobbitt, K. L.; Maloney, V. M.; Gaspar, P. P. *Organometallics* **1991**, *10*, 2772–2777.

19. Nakayama, S.; Yoshifuji, M.; Okazaki, R.; Inamoto, O. *J. Chem. Soc., Chem. Commun.* **1971**, 1186–1187.

20. Yoshifuji, M.; Nakayama, S.; Okazaki, R.; Inamoto, N. *J. Chem. Soc., Perkin Trans. I.* **1973**, 2065–2068.

21. Nakayama, S.; Yoshifuji, M.; Okazaki, R.; Inamoto, N. *J. Chem. Soc., Perkin Trans. I.* **1973**, 2069–2071.

22. Nakayama, S.; Yoshifuju, M.; Okazaki, R.; Inamoto, N. *Bull. Chem. Soc. Jpn.* **1975**, *48*, 546–548.

23. Stille, J. K.; Eichelberger, J. L.; Higgins, J.; Freeburger, M. E. *J. Am. Chem. Soc.* **1972**, *94*, 4761–4763.

24. Tomioka, H.; Hirano, Y.; Izawa, Y. *Tetrahedron Lett.* **1974**, 1865–1866.

25. Tomioka, H.; Izawa, Y. *J. Org. Chem.* **1977**, *42*, 582–584.

26. Tomioka, H.; Hirano, Y.; Izawa, Y. *Tetrahedron Lett.* **1974**, 4477–4478.

27. Santini, C. C.; Fischer, J.; Mathey, F.; Mitschler, A. *J. Am. Chem. Soc.* **1980**, *102*, 5809–5815.

28. Holand, S.; Mathey, F. *J. Org. Chem.* **1981**, *46*, 4386–4389.

29. Tomioka, H.; Miura, S.; Izawa, Y. *Tetrahedron Lett.* **1983**, *24*, 3353–3356.
30. Quin, L. D.; Jankowski, S.; Rudzinski, J.; Sommese, A. G.; Wu, X.-P. *J. Org. Chem.* **1993**, *58*, 6212–6216.
31. Quast, H.; Heuschmann, M. *Angew. Chem., Int. Ed. Engl.* **1978**, *17*, 867–868.
32. Quast, H.; Heuschmann, M. *Ann. Chem.* **1981**, 977–992.
33. Quast, H.; Heuschmann, M. *Chem. Ber.* **1982**, *115*, 901–909.
34. Quin, L. D.; Yao, E. U.; Szewczyk, J. *Tetrahedron Lett.* **1987**, *28*, 1077–1080.
35. Yoshifuji, M.; Hirano, M.; Toyota, K. *Tetrahedron Lett.* **1993**, *34*, 1043–1046.
36. Yoshifuji, M.; Sangu, S.; Hirano, M.; Toyota, K. *Chem. Lett.* **1993**, 1715–1718.
37. Cowley, A. H.; Gabbaï, F. P.; Corbelin, S.; Decken, A. *Inorg. Chem.* **1995**, *34*, 5931–5932.
38. Qian, H.; Gaspar, P. P.; Rath, N. P. *J. Organomet. Chem.* **1999**, *585*, 167–173.
39. Li, X.; Robinson, K. D.; Gaspar, P. P. *J. Org. Chem.* **1996**, *61*, 7702–7710.
40. Oshikawa, T.; Yamashita, M. *Synthesis.* **1985**, 290–291.
41. At the lowest temperature employed, 44°C, the disappearance of **14** was monitored for only one half-life due to the slowness of the reaction.
42. Direct RHF calculations were carried out employing the Spartan molecular modeling program (Wavefunction, Inc.) version 5.0. Geometry optimization of 1-methylphosphirane oxide at HF/6-31G* (Fig. 8(a)) yielded $E=-533.236467$ hartrees. The transition state for pyrolysis of 1-methylphosphirane oxide to C_2H_4 and Me–P=O (Fig. 8(b)), $E=-533.169997$ hartrees, was found by optimization at HF/6-31G* of the structure of maximum energy at AM1 upon stretching a ring P–C bond of methylphosphirane oxide. Vibrational frequencies were calculated by numerical differentiation of analytical gradients using central differences. The transition state has one imaginary vibration that indicated that it is on the correct reaction path. Molecular entropies were calculated using unscaled frequencies.
43. Wolf, R.; Houalla, D.; Mathis, F. *Spectrochim. Acta, Part A* **1967**, *23*, 1641–1656.
44. Gruneich, J. A.; Wisian-Neilson, P. *Macromolecules* **1996**, *29*, 5511–5512.
45. Monkiewicz, J.; Pietrusiewicz, K. M.; Bodalski, R. *Bull. Acad. Pol. Sci. Ser. Sci. Chim.* **1980**, *28*, 351.
46. Summers, M. F.; Marzilli, L. G.; Bax, A. *J. Am. Chem. Soc.* **1986**, *108*, 4285–4294.
47. Keating, A. E.; Merrigan, S. R.; Singleton, D. A.; Houk *J. Am. Chem. Soc.* **1999**, *121*, 3933–3938.
48. Popoff, C. M.; Berry, D. H. manuscript in preparation, private communication from D. H. Berry with permission to quote.
49. Mathey, F. Phosphinidenes. *Multiple Bonds and Low Coordination in Phosphorus Chemistry*; Regitz, M., Scherer, O. J. Eds.; Georg Thieme: Stuttgart, 1990, pp 33–47.
50. Corey, E. J.; Mitra, R. B. *J. Am. Chem. Soc.* **1962**, *84*, 2938–2941.
51. Qian, H. *Synthesis of Small Ring Phosphorus Heterocycles and their Chemistry*, Washington University: St. Louis, December 1998.